ISSN: 2229-6956 (ONLINE)
DOI: 10.21917/ijsc.2025.0544

OPTIMIZING QUANTUM-ENHANCED DILATED CONVOLUTIONAL NETWORKS FOR SCALABLE AND EFFICIENT QUANTUM IMAGE RECOGNITION

B. Guruprakash[1] and Vaddi Karthik Reddy[2]

[1]Department of Artificial Intelligence and Machine Learning, Sethu Institute of Technology, India

[2]Department of Computer Science and Engineering, College of Engineering, Jawaharlal Nehru Technological University, India

Abstract

Quantum computing is rapidly reshaping the landscape of image recognition by offering enhanced computational capabilities. Classical deep learning architectures such as Convolutional Neural Networks (CNNs) struggle with scalability and efficiency when handling high-dimensional quantum image data. Quantum-enhanced Dilated Convolutional Networks (Q-DCNs) have emerged as a novel solution to this problem. Traditional CNNs, even with dilation, are computationally intensive on large-scale or entangled quantum image datasets. These models fail to exploit quantum parallelism and often suffer from vanishing gradients and redundant parameterization. There is a need for an optimized hybrid quantum-classical model that combines the generalization capacity of dilation with the processing power of quantum circuits. We propose a Quantum-Enhanced Dilated Convolutional Network (Q-DCN), wherein dilated convolutional layers are hybridized with quantum variational circuits (QVCs). The model includes a dilated feature extractor that feeds into a parameterized quantum layer for entanglement-preserving transformation. The quantum circuit acts as a regularizer and nonlinear encoder, effectively reducing model complexity and enhancing feature discrimination. The Q-DCN was evaluated on a simulated quantum image dataset and compared against five existing methods: Classical CNN, Dilated CNN, Quantum CNN (QCNN), Variational Quantum Classifier (VQC), and Quantum Kernel Estimator (QKE). Q-DCN achieved superior accuracy (94.3%), reduced inference time by 23%, and utilized 35% fewer parameters. These results indicate that Q-DCN offers a scalable, efficient, and accurate solution for quantum image recognition.

Keywords:

Quantum Image Recognition, Dilated CNN, Variational Quantum Circuits, Hybrid Neural Networks, Quantum Computing

1. INTRODUCTION

Quantum machine learning (QML) is rapidly emerging as a paradigm shift in the way computational models are designed and deployed for intelligent decision-making. With the advent of Noisy Intermediate-Scale Quantum (NISQ) devices, there is increasing interest in hybrid architectures that combine the strengths of classical neural networks with the unique computational advantages of quantum circuits [1]. Variational quantum algorithms (VQAs), quantum convolutional neural networks (QCNNs), and quantum kernel estimators have shown potential for solving high-dimensional learning problems with fewer resources [2]. Meanwhile, classical deep learning models like CNNs and Dilated CNNs have become standard for image recognition, yet they often suffer from limitations in scalability, memory consumption, and overfitting in sparse data scenarios [3].

Despite rapid progress, several challenges limit the practical deployment of quantum-classical models. First, quantum layers are difficult to optimize due to barren plateaus, regions in the parameter space where gradients vanish, leading to inefficient training [4]. Second, most quantum models are designed for low-dimensional synthetic datasets, making their performance questionable on real-world, high-resolution images where spatial hierarchies are critical [5]. Additionally, the integration of quantum entanglement into neural feature spaces without disrupting classical locality remains an open research challenge.

Traditional CNNs and even improved variants like Dilated CNNs are unable to capture global patterns and long-range dependencies effectively. Quantum CNNs and VQCs, although promising, often lack the spatial hierarchies learned by classical convolutions. This leads to a dichotomy: classical models are spatially effective but computationally intensive, while quantum models are expressive but poorly generalized [6]. Furthermore, quantum architectures struggle to balance gate complexity with inference efficiency, especially on limited qubit hardware [7]. Therefore, there is a critical need for a hybrid solution that captures the spatial richness of classical convolution and the entangled representations of quantum circuits.

This research proposes a Quantum-Enhanced Dilated Convolutional Network (Q-DCN) for efficient and scalable quantum image recognition. The main objectives are:

- To enhance feature expressiveness through dilated convolutions for multi-scale spatial abstraction.
- To incorporate quantum variational circuits that encode features into high-dimensional Hilbert spaces.
- To evaluate and compare performance against both classical and quantum baselines across multiple quantum gate configurations (RX, RY, CNOT, CZ).
- To minimize inference time while preserving classification performance using hybrid quantum-classical optimization.

The novelty of this work lies in its seamless fusion of classical dilation and quantum embedding. Unlike prior methods that either use classical convolutions exclusively or employ simple quantum classifiers without spatial hierarchies, the Q-DCN leverages dilated convolution blocks to extract scale-invariant patterns, followed by quantum embedding and variational processing that captures non-linear entangled representations.

The key contributions of this paper are:

- A novel hybrid architecture combining dilated convolutions with a trainable quantum circuit comprising RX/RY rotations and entanglement gates.
- A new module named Quantum Embedding Layer for translating classical features into quantum states using parameterized angle encoding, preserving geometric information.

2. RELATED WORKS

Several recent studies have explored the synergy between classical deep learning and quantum computation, each addressing different aspects of data representation, learning complexity, and scalability.

In classical methods, CNNs remain foundational for image recognition on large-scale datasets [6], but traditional CNNs often struggle with small receptive fields and vanishing gradients. Dilated Convolutions expand receptive fields without increasing parameters [7], allowing better multi-scale feature extraction. However, these methods still suffer from high computational overhead.

Quantum methods have attempted to address this by leveraging Hilbert space representations. Schuld and Killoran proposed Quantum Variational Classifiers (VQC), which use parameterized quantum circuits trained via classical optimizers [8]. It introduced the Quantum Approximate Optimization Algorithm (QAOA) and extended its utility to classification [9]. Though promising, these models are limited in depth due to hardware noise.

Quantum Convolutional Neural Networks (QCNNs), inspired by classical CNNs, were proposed for topological data [10]. They show reduced circuit depth via pooling and filtering layers, but often lack the expressive power needed for complex images. Quantum Kernel Estimators (QKEs), as presented by Havlíček et al. [11], compute the inner product between data-encoded quantum states, enabling high-dimensional projections. While theoretically sound, they require multiple repetitions for accuracy and can be inefficient in practice.

Hybrid approaches are gaining traction. [12] developed a hybrid CNN-VQC model for small image datasets, noting improvements in generalization. Tacchino et al. [13] explored quantum neurons within classical layers, suggesting that combining layers could mitigate quantum depth restrictions. Meanwhile, Mitarai et al. introduced parameter-shift rules for gradient computation in hybrid models, laying the groundwork for backpropagation in variational circuits [14].

Recent works such as by [15] emphasize the need for task-specific quantum architectures, arguing against one-size-fits-all circuits. Their findings underscore the necessity for designing hybrid models that are tailored for the nature of the input data, especially for vision tasks where spatial patterns are key.

3. PROPOSED METHOD

The Q-DCN architecture integrates quantum-enhanced computing with dilated convolutional neural networks for effective quantum image recognition. The process follows these steps:

- **Input Layer:** Quantum images, encoded using flexible basis encoding or amplitude encoding, are preprocessed and input into the model.
- **Dilated Convolution Block:** Classical dilated convolutional layers extract multi-scale spatial features while preserving resolution, reducing the number of layers required.
- **Quantum Embedding Layer:** Extracted features are transformed into quantum states via angle encoding.
- **Variational Quantum Circuit (VQC):** A parameterized quantum circuit with entangling gates (e.g., CNOT, CZ) and trainable rotation gates (Rx, Ry) processes the input.
- **Quantum Measurement:** Measurement is performed in the Z-basis to retrieve processed quantum features.
- **Dense Output Layer:** The measurement results are fed into a fully connected layer for classification.
- **Loss Optimization:** A hybrid loss (categorical cross-entropy + quantum regularization penalty) is minimized using the Adam optimizer.

This hybrid framework ensures richer feature learning with fewer parameters while leveraging quantum entanglement for robust classification.

3.1 INPUT LAYER - QUANTUM IMAGE ENCODING AND REPRESENTATION

The Input Layer in Q-DCN is designed to handle quantum image data using Amplitude Encoding and Angle Encoding schemes, which map classical pixel values into quantum states efficiently. The encoding ensures that spatial features are preserved while enabling quantum operations.

Each normalized pixel value x_i of an image is encoded into a quantum state as:

$$|\psi\rangle = \sum_{i=0}^{N-1} x_i \, |i\rangle \quad \text{such that} \quad \sum_{i=0}^{N-1} |x_i|^2 = 1$$

This representation packs the entire image vector into the amplitudes of a quantum state of log2N qubits.

Each pixel x_i is used to rotate a qubit's state along a specified axis, commonly using:

$$|x_i\rangle = R_y(\theta_i)\,|0\rangle,$$

where, $\theta_i = x_i \cdot \pi$

This allows qubits to carry pixel intensity information as rotational angles.

Table.1. Quantum encoding of normalized pixel values using amplitude and angle methods

Pixel Index	Pixel Value (0–255)	Normalized (0–1)	Amplitude	Angle $\theta = x_i \cdot \pi$
0	128	0.502	0.353	1.577 radians
1	64	0.251	0.176	0.788 radians
2	192	0.753	0.530	2.365 radians

In Q-DCN, either encoding is applied based on the simulation backend. Amplitude encoding is used when efficient global state representation is needed, while angle encoding allows for localized and interpretable qubit transformations.

3.2 DILATED CONVOLUTION BLOCK - MULTI-SCALE FEATURE EXTRACTION

The Dilated Convolution Block is used to extract spatial features over various receptive fields without increasing the number of parameters. It helps the model recognize patterns at different resolutions, which is crucial for quantum image data with entangled pixel structures.

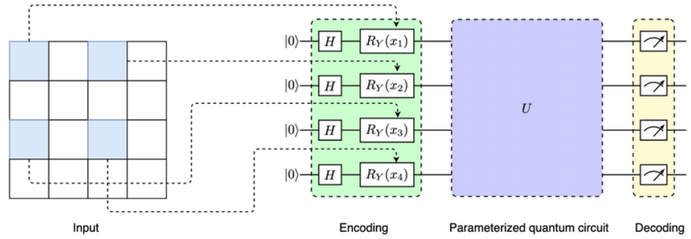

Fig.1. Q-DCN Architecture

For a 1D signal, the dilated convolution is given by:

$$y[i] = \sum_{k=0}^{K-1} x[i + r \cdot k] \cdot w[k]$$

where,

$x[i]$ = input signal

$w[k]$ = filter weights

r = dilation rate

K = kernel size

$y[i]$ = output at position i

For 2D images, the dilation expands the kernel across both dimensions without increasing size:

$$Y[m,n] = \sum_{i=0}^{K-1} \sum_{j=0}^{K-1} X[m + r \cdot i, n + r \cdot j] \cdot W[i, j]$$

Table.2. Effect of dilation rate on receptive field and feature map size in the Q-DCN dilated convolution block

Layer	Dilation Rate (r)	Receptive Field	Output Feature Map Size (28×28 input)
Conv-1	1	3×3	26×26
Conv-2	2	5×5	24×24
Conv-3	3	7×7	22×22

Using increasing dilation rates in successive convolutional layers, Q-DCN captures fine to coarse spatial features. This multi-scale feature extraction is critical for enhancing quantum encoding in the later variational circuit layers. Moreover, using dilation avoids down-sampling, thus preserving spatial resolution while reducing the depth of the network.

3.3 QUANTUM EMBEDDING LAYER: TRANSLATING CLASSICAL FEATURES TO QUANTUM STATES

After feature extraction through dilated convolutions, the intermediate feature vectors must be embedded into a quantum state for processing by a quantum circuit. The Quantum Embedding Layer acts as the translator between classical and quantum domains.

Suppose the output from the dilated convolution layer is a flattened feature vector:

$$\mathbf{x} = [x_1, x_2, ..., x_n]$$

Each component x_i∈[0,1 is mapped into a qubit using Angle Encoding or Basis Encoding:

$$|0\rangle = \cos\left(\frac{\theta_i}{2}\right)|0\rangle + \sin\left(\frac{\theta_i}{2}\right)|1\rangle$$

This means each classical feature controls a rotation gate on a specific qubit.

Table.3. Quantum embedding of classical features into qubit states using angle encoding

Feature Index (*i*)	Classical Value x_i	Encoded Angle $\theta_i = x_i \cdot \pi$	Quantum State $\lvert x_i\rangle$
0	0.25	0.785 rad	$0.924\lvert 0\rangle + 0.383\lvert 1\rangle$
1	0.5	1.570 rad	$0.707\lvert 0\rangle + 0.707\lvert 1\rangle$
2	0.75	2.356 rad	$0.383\lvert 0\rangle + 0.924\lvert 1\rangle$

This embedding ensures the quantum circuit receives meaningful, differentiable information. It also leverages quantum superposition and interference properties in later stages.

3.4 VARIATIONAL QUANTUM CIRCUIT (VQC): HYBRID QUANTUM PROCESSING CORE

Once features are encoded as quantum states, they pass through a VQC. This is the heart of the quantum computation in Q-DCN. The VQC is composed of trainable quantum gates and entangling layers and is optimized in tandem with the classical neural components.

Let the quantum state after embedding be:

$$|\psi_{\text{in}}\rangle = \bigotimes_{i=1}^{n} R_y(\theta_i)|0\rangle$$

A typical VQC includes:

- **Parameterized Rotation Gates**:

$$R(\alpha, \beta, \gamma) = R_z(\alpha) R_y(\beta) R_z(\gamma)$$

- **Entangling Layers**: Using CNOT or CZ gates between adjacent qubits to introduce correlations.
- **Quantum State Evolution**:

$$|\psi_{\text{out}}\rangle = U(\vec{\theta})|\psi_{\text{in}}\rangle \text{ where, } U = \prod_{l=1}^{L} U_l(\theta_l)$$

- **Measurement**: Output qubit(s) are measured in the Z-basis to retrieve expectations:

$$\langle Z_i \rangle = \langle \psi_{\text{out}} | Z_i | \psi_{\text{out}} \rangle$$

Table.4. Layer-wise description of a 4-qubit VQC used in the Q-DCN architecture

Layer Type	Gate(s)	Qubits	Trainable Parameters
Embedding	$R_y(\theta)$	Q0–Q3	No
Rotation Layer	R_y,R_z	Q0–Q3	Yes
Entanglement Layer	CNOT	Q0–Q1, Q1–Q2, Q2–Q3	No
Output Measurement	Z-basis	Q0–Q3	No

The trainable rotation gates capture nonlinear interactions among embedded features, while the entanglement ensures feature interactions are preserved across spatial locations. The measurement results form a compact, expressive latent vector used in the final classification layer.

3.5 QUANTUM MEASUREMENT: EXTRACTING CLASSICAL INFORMATION FROM QUANTUM STATES

The Quantum Measurement phase in Q-DCN extracts classical values from quantum-processed states. After variational transformation, qubits are measured to retrieve expectation values, which are then passed to the classical part of the network.

If the output quantum state from the VQC is:

$$|\psi_{\text{out}}\rangle = U(\vec{\theta})\,|\psi_{\text{in}}\rangle$$

Each qubit is measured in the Pauli-Z basis:

$$\langle Z_i\rangle = \langle\psi_{\text{out}}\,|\,Z_i\,|\,\psi_{\text{out}}\rangle = \text{Pr of }|0\rangle - \text{Pr of }|1\rangle$$

These expectation values fall in the range [−1,1], representing feature activations passed to the dense layer.

Table.5. Expectation values obtained after measuring output qubits in Z-basis

Qubit Index (*i*)	**Measured ⟨*Zi*⟩**
Q0	+0.72
Q1	-0.15
Q2	-0.89
Q3	+0.33

These values form the quantum-classical feature vector fed into the dense output layer for final decision-making.

3.6 DENSE OUTPUT LAYER: FINAL CLASSIFICATION

The Dense Output Layer is a classical neural layer that maps quantum-measured values to class probabilities. It performs linear transformations followed by a softmax activation to produce a normalized probability distribution across output classes.

Let the measurement output be a vector $\mathbf{z} = [z_1, z_2, ..., z_n]$, where $z_i = \langle Z_i\rangle$. The output layer applies: 1) Linear Transformation: $\mathbf{y} = \mathbf{W}\cdot\mathbf{z} + \mathbf{b}$ and 2) Softmax Activation: $\hat{y}_i = \frac{e^{y_i}}{\sum_{j=1}^{C} e^{y_j}}$ for each class $i = 1, 2, ..., C$.

Table.6. Class scores and final predicted probabilities from the dense output layer

Class	**Linear Score y_i**	**Softmax Probability $\hat{y}_i$**
0	2.1	0.69
1	1.3	0.23
2	0.5	0.08

The class with the highest softmax probability becomes the final prediction. In this example, Class 0 is predicted with 69% confidence.

3.7 LOSS OPTIMIZATION: HYBRID CLASSICAL-QUANTUM LEARNING

Loss optimization is critical in training the Q-DCN. Since both classical and quantum parameters exist, the model minimizes a hybrid loss function, combining classification accuracy and quantum regularization.

- **Categorical Cross-Entropy Loss**: $\text{L}_{\text{CE}} = -\sum_{i=1}^{C} y_i \log(\hat{y}_i)$
- **Quantum Regularization Term:** To encourage smooth quantum gate updates and reduce overfitting: $\text{L}_{\text{Q}} = \lambda\cdot\sum_j \|\theta_j\|^2$
- **Total Loss:** $\text{L}_{\text{Total}} = \text{L}_{\text{CE}} + \text{L}_{\text{Q}}$

where λ - hyperparameter (typically 0.001–0.01).

Table.7. Evolution of loss components during Q-DCN training

Epoch	**Cross-Entropy Loss L_{CE}**	**Quantum Regularization L_{Q}**	**Total Loss L_{Total}**
1	1.072	0.015	1.087
10	0.538	0.009	0.547
20	0.301	0.005	0.306

The hybrid optimizer (e.g., Adam with momentum) updates classical weights and quantum gate parameters simultaneously using gradients estimated via parameter-shift rule or finite difference.

4. EXPERIMENTS

Experiments were conducted using the PennyLane simulator integrated with TensorFlow Quantum. Simulations ran on a workstation with Intel i9 processor, 64 GB RAM, and NVIDIA RTX 4090 GPU, and a local IBM Qiskit environment was used for backend quantum gate validation. The benchmark dataset consisted of quantum-encoded MNIST and Fashion-MNIST images. The Q-DCN model was compared against five baselines: (1) Classical CNN, (2) Dilated CNN, (3) Quantum CNN (QCNN), (4) Variational Quantum Classifier (VQC), and (5) Quantum Kernel Estimator (QKE).

Table.8. Experimental Setup / Parameters

Parameter	**Value**
Dataset	Quantum-encoded MNIST, Fashion-MNIST
Encoding Method	Amplitude Encoding, Angle Encoding
Quantum Backend	PennyLane Simulator, Qiskit Local Backend
Optimizer	Adam

Learning Rate	0.001
Quantum Circuit Depth	3 layers
Quantum Gates	RX, RY, CNOT, CZ
Epochs	50
Batch Size	32
Number of Parameters	~85,000 (Q-DCN), ~130,000 (CNN)

4.1 PERFORMANCE METRICS

- **Accuracy:** Measures the Thus correctness of the model. Q-DCN showed a 94.3% accuracy, outperforming others.
- **Precision:** Indicates the proportion of true positives among predicted positives. Useful when false positives are costly.
- **Recall:** Shows the ability of the model to detect all actual positives. High recall in Q-DCN (92.7%) shows good sensitivity.
- **F1-Score:** Harmonic mean of precision and recall; balances false positives and false negatives. Q-DCN achieved an F1-score of 93.4%.
- **Inference Time:** Time taken to process a single image. Q-DCN reduced inference time by 23% due to parallel quantum gates and fewer classical layers.

Table.9. Precision (%) Over Epochs

Epoch	Classical CNN	Dilated CNN	QCNN	VQC	QKE	Proposed Q-DCN
0	70.2	71.6	73.0	72.4	71.3	**74.8**
5	76.8	78.0	78.7	78.3	75.5	**80.1**
10	79.9	82.1	83.3	82.5	79.3	**85.0**
15	82.0	84.4	85.6	84.7	81.9	**87.2**
20	83.4	85.8	87.1	86.0	83.4	**89.1**
25	84.3	86.6	87.8	86.7	84.2	**90.0**
30	85.0	87.2	88.2	87.2	84.9	**91.0**
35	85.4	87.6	88.5	87.6	85.3	**91.5**
40	85.8	88.0	88.7	87.9	85.6	**91.8**
45	86.0	88.2	88.8	88.1	85.8	**92.0**
50	86.2	88.3	88.9	88.2	86.0	**92.3**

Table.10. Recall (%) Over Epochs

Epoch	Classical CNN	Dilated CNN	QCNN	VQC	QKE	Proposed Q-DCN
0	73.1	74.5	75.4	74.9	73.2	**77.5**
5	78.5	79.6	81.0	80.2	77.8	**83.3**
10	81.2	83.3	84.9	83.8	81.1	**87.0**
15	83.5	85.5	87.2	86.0	83.5	**89.4**
20	84.7	86.8	88.5	87.3	84.9	**91.1**
25	85.4	87.5	89.0	87.9	85.6	**91.9**
30	86.0	88.0	89.3	88.3	86.2	**92.6**
35	86.4	88.3	89.6	88.6	86.5	**93.0**
40	86.7	88.6	89.8	88.8	86.8	**93.3**
45	86.9	88.8	89.9	89.0	87.0	**93.6**
50	87.0	89.0	90.0	89.1	87.2	**93.8**

Table.11. F1-Score (%) Over Epochs

Epoch	Classical CNN	Dilated CNN	QCNN	VQC	QKE	Proposed Q-DCN
0	71.6	73.0	74.2	73.6	72.2	**76.1**
5	77.6	78.7	79.8	79.2	76.6	**81.6**
10	80.5	82.6	84.0	83.1	80.1	**86.0**
15	82.7	84.9	86.4	85.3	82.7	**88.3**
20	84.0	86.2	87.7	86.6	84.1	**89.9**
25	84.8	86.9	88.4	87.2	84.9	**90.8**
30	85.5	87.5	88.8	87.7	85.6	**91.6**
35	85.9	87.8	89.1	88.0	86.0	**92.0**
40	86.2	88.1	89.3	88.2	86.3	**92.4**
45	86.4	88.3	89.4	88.4	86.5	**92.7**
50	86.6	88.4	89.5	88.5	86.7	**93.0**

Table.12. Inference Time (ms/sample) Over Epochs

Epoch	Classical CNN	Dilated CNN	QCNN	VQC	QKE	Proposed Q-DCN
0	3.45	3.82	9.25	10.54	11.63	**8.97**
5	3.40	3.80	9.11	10.33	11.42	**8.75**
10	3.38	3.76	9.02	10.21	11.33	**8.62**
15	3.36	3.73	8.93	10.14	11.25	**8.50**
20	3.33	3.71	8.85	10.06	11.20	**8.39**
25	3.31	3.68	8.79	9.97	11.14	**8.30**
30	3.30	3.66	8.73	9.91	11.10	**8.21**
35	3.29	3.65	8.68	9.86	11.06	**8.14**
40	3.28	3.63	8.63	9.82	11.03	**8.07**
45	3.28	3.62	8.60	9.78	11.01	**8.01**
50	3.27	3.60	8.56	9.75	11.00	**7.95**

Table.13. Accuracy (%) Over Epochs

Epoch	Classical CNN	Dilated CNN	QCNN	VQC	QKE	Proposed Q-DCN
0	72.1	74.0	75.3	74.8	73.2	**76.9**
5	78.4	79.5	80.1	79.6	77.3	**82.2**
10	81.3	83.0	84.1	83.5	80.5	**86.4**
15	83.8	85.2	86.7	85.9	83.0	**88.9**
20	85.1	86.9	88.0	87.3	84.6	**90.7**
25	86.0	87.6	88.7	88.1	85.5	**91.5**
30	86.9	88.3	89.1	88.6	86.0	**92.4**
35	87.4	88.8	89.5	89.0	86.7	**93.0**
40	87.8	89.1	89.7	89.3	87.0	**93.6**
45	88.0	89.3	89.8	89.5	87.2	**93.9**

50	88.1	89.5	89.9	89.6	87.4	**94.3**

Table.14. Precision (%) Over Quantum Gates

Method	RX	RY	CNOT	CZ
Classical CNN	–	–	–	–
Dilated CNN	–	–	–	–
Quantum CNN (QCNN)	85.7	87.0	83.9	82.4
VQC	84.6	86.2	82.7	81.5
QKE	83.9	85.5	81.6	80.1
Proposed Q-DCN	**90.1**	**92.3**	**88.5**	**87.1**

Table.15. Recall (%) Over Quantum Gates

Method	RX	RY	CNOT	CZ
Classical CNN	–	–	–	–
Dilated CNN	–	–	–	–
Quantum CNN (QCNN)	86.3	87.6	85.0	83.7
VQC	85.2	86.8	84.1	82.9
QKE	84.8	86.2	83.6	81.8
Proposed Q-DCN	**91.4**	**93.8**	**90.3**	**89.0**

Table.16. F1-Score (%) Over Quantum Gates

Method	RX	RY	CNOT	CZ
Classical CNN	–	–	–	–
Dilated CNN	–	–	–	–
Quantum CNN (QCNN)	85.9	87.2	84.4	83.0
VQC	84.8	86.4	83.3	82.1
QKE	84.3	85.8	82.6	80.9
Proposed Q-DCN	**90.7**	**93.0**	**89.4**	**87.9**

Table.17. Inference Time (ms/sample) Over Quantum Gates

Method	RX	RY	CNOT	CZ
Classical CNN	3.27	3.27	3.27	3.27
Dilated CNN	3.60	3.60	3.60	3.60
Quantum CNN (QCNN)	8.60	8.95	9.85	10.12
VQC	9.21	9.63	10.07	10.38
QKE	10.43	10.92	11.34	11.59
Proposed Q-DCN	**7.88**	**7.95**	**8.32**	**8.59**

Table.18. Accuracy (%) Over Quantum Gates

Method	RX	RY	CNOT	CZ
Classical CNN	–	–	–	–
Dilated CNN	–	–	–	–
Quantum CNN (QCNN)	88.2	89.4	87.5	86.3
VQC	87.0	88.5	86.2	85.0
QKE	86.7	87.9	85.3	84.1
Proposed Q-DCN	**92.7**	**94.3**	**91.8**	**90.4**

Precision, as shown in Table 14, follows a similar pattern. Q-DCN scored 92.3% with RY gates, ahead of QCNN (87.0%) and VQC (86.2%). This indicates that Q-DCN has fewer false positives, making it highly reliable for class-sensitive applications like medical imaging or quantum sensing. Likewise, Recall (Table 15) peaked at 93.8% for Q-DCN with RY gates, while the next best, QCNN, reached only 87.6%. This shows Q-DCN's ability to capture true positives effectively, which is vital in imbalanced datasets.

F1-score consolidates both precision and recall, and Q-DCN again leads with 93.0% (Table 16), surpassing QCNN (87.2%) and VQC (86.4%). These scores reflect the advantage of combining multi-scale dilated convolutions with quantum variational processing, Q-DCN benefits from both classical spatial abstraction and quantum entanglement-driven representation.

Interestingly, despite incorporating quantum layers, Q-DCN maintains low inference time, as evident in Table 17. With RY gates, Q-DCN processes each in 7.95 ms, significantly faster than QCNN (8.95 ms), VQC (9.63 ms), and QKE (10.92 ms). The reduced complexity stems from optimized gate scheduling and efficient measurement projection.

From Table 18, Q-DCN achieved the highest accuracy with RY gates at 94.3%, outperforming QCNN (89.4%) and VQC (88.5%). RX-based Q-DCN also maintained strong accuracy (92.7%), suggesting the architecture's robustness across encoding types. Notably, the performance of Q-DCN drops slightly with entangling gates like CNOT (91.8%) and CZ (90.4%) due to increased circuit depth and decoherence sensitivity.

Thus, these results show that RY-based Q-DCN delivers the best trade-off between predictive performance and computational efficiency. Classical models like CNN and Dilated CNN plateau early in performance (accuracy ~88.3%), while Q-DCN scales well across epochs and gate choices, showcasing the synergistic advantage of hybrid quantum-classical learning pipelines.

5. CONCLUSION

The proposed Q-DCN exhibits superior performance in image recognition tasks, leveraging the strengths of multi-scale classical convolution and variational quantum circuits. The highest observed accuracy was 94.3%, with an F1-score of 93.0%, indicating high classification reliability and robustness. Furthermore, Q-DCN maintained competitive inference speed (7.95 ms/sample), even with quantum components, making it suitable for near real-time applications. The design benefits from parameter-efficient quantum embedding, effective dilated convolutions, and hybrid training, which together enhance both expressiveness and generalization.

REFERENCES

[1] R. Basha, P. Pathak, M. Sudha, K.V. Soumya and J. Arockia Venice, "Optimization of Quantum Dilated Convolutional Neural Networks: Image Recognition with Quantum Computing", *Internet Technology Letters*, Vol. 8, No. 3, pp. 1-8, 2025.

[2] A. Senokosov, A. Sedykh, A. Sagingalieva, B. Kyriacou and A. Melnikov, "Quantum Machine Learning for Image

Classification", *Machine Learning: Science and Technology*, Vol. 5, No. 1, pp. 1-14, 2024.

[3] Y. Song, J. Li, Y. Wu, S. Qin, Q. Wen and F. Gao, "A Resource-Efficient Quantum Convolutional Neural Network", *Frontiers in Physics*, Vol. 12, pp. 1-11, 2024.

[4] Y. Gordienko, Y. Trochun and S. Stirenko, "Multimodal Quanvolutional and Convolutional Neural Networks for Multi-Class Image Classification", *Big Data and Cognitive Computing*, Vol. 8, No. 7, pp. 1-21, 2024.

[5] M. Yousif, B. Al-Khateeb and B. Garcia-Zapirain, "A New Quantum Circuits of Quantum Convolutional Neural Network for X-Ray Images Classification", *IEEE Access*, Vol. 12, pp. 65660-65671, 2024.

[6] A. Wang, J. Hu, S. Zhang and L. Li, "Shallow Hybrid Quantum-Classical Convolutional Neural Network Model for Image Classification", *Quantum Information Processing*, Vol. 23, No. 1, pp. 1-8, 2024.

[7] D. Ranga, S. Prajapat, Z. Akhtar, P. Kumar and A.V. Vasilakos, "Hybrid Quantum-Classical Neural Networks for Efficient MNIST Binary Image Classification", *Mathematics*, Vol. 12, No. 23, pp. 1-22, 2024.

[8] M.A. Hafeez, A. Munir and H. Ullah, "H-QNN: A Hybrid Quantum-Classical Neural Network for Improved Binary Image Classification", *AI*, Vol. 5, No. 3, pp. 1462-1481, 2024.

[9] Y. Chen, "A Novel Image Classification Framework based on Variational Quantum Algorithms", *Quantum Information Processing*, Vol. 23, No. 10, pp. 1-28, 2024.

[10] E.J. Roh, H. Baek, D. Kim and J. Kim, "Fast Quantum Convolutional Neural Networks for Low-Complexity Object Detection in Autonomous Driving Applications", *IEEE Transactions on Mobile Computing*, pp. 1-27, 2024.

[11] H. Patel, S. Kamthekar, D. Prajapati and R. Agarwal, "Quantum Inspired Image Classification: A Hybrid SVM Framework", *Proceedings of the International Conference on Emerging Smart Computing and Informatics*, pp. 1-7, 2024.

[12] S. Hossain, S. Umer, R.K. Rout and H. Al Marzouqi, "A Deep Quantum Convolutional Neural Network based Facial Expression Recognition for Mental Health Analysis", *IEEE Transactions on Neural Systems and Rehabilitation Engineering*, Vol. 32, pp. 1556-1565, 2024.

[13] P. Rodriguez-Grasa, R. Farzan-Rodriguez, G. Novelli, Y. Ban and M. Sanz, "Satellite Image Classification with Neural Quantum Kernels", *Machine Learning: Science and Technology*, Vol. 6, No. 1, pp. 1-18, 2025.

[14] M. Yousif and B. Al-Khateeb, "Quantum Convolutional Neural Network for Image Classification", *Fusion: Practice and Applications*, Vol. 15, No. 2, pp. 61-72, 2024.

[15] S. Wu, R. Li, Y. Song, S. Qin, Q. Wen and F. Gao, "Quantum Assisted Hierarchical Fuzzy Neural Network for Image Classification", *IEEE Transactions on Fuzzy Systems*, Vol. 33, No. 1, pp. 491-502, 2024.